Ultrafast absorber saturation process and short pulse formation in injection lasers

S. V. Zaitsev, N. Yu. Gordeev, and M. P. Soshnikov
Ioffe Physicotechnical Institute, Russian Academy of Sciences, St. Petersburg, Russia

J. S. Massa and G. S. Buller[a)]
Department of Physics, Heriot–Watt University, Riccarton, Edinburgh EH14 4AS, United Kingdom

(Received 23 February 1998; accepted for publication 15 August 1998)

The nature of lasing threshold in passively *Q*-switched GaAs/AlGaAs lasers with saturable absorbers formed by heavy ion implantation is investigated in this article. After studying various laser characteristics, including threshold current density, differential quantum efficiency, spectral output, and picosecond time-resolved emission, we conclude that the origin of the *Q*-switching is unlikely to be caused by spontaneous emission or mode locking, and that collective coherent radiation effects may contribute to the onset of lasing. © *1998 American Institute of Physics.* [S0021-8979(98)03422-7]

INTRODUCTION

There have been numerous publications concerning semiconductor injection lasers containing saturable absorber sections.[1,2] One successful method of forming the saturable absorber section is heavy ion bombardment of the facets.[3,4] Semiconductor lasers of this type have been fabricated from AlGaAs/GaAs double heterostructures (DHs), as well as from InGaAsP/InP DHs.[5] These lasers have proved capable of emitting ultrashort optical pulses when used in the *Q*-switching regime. Typical results for AlGaAs/GaAs lasers have given ~10 pJ in a 10 ps optical pulse. In this article the origin of the *Q*-switched pulse formation in such lasers is investigated. A greater understanding of the underlying physical processes which enable initiation of *Q*-switching in such lasers could lead to improved jitter and current threshold levels in all *Q*-switched semiconductor lasers. On a more general level, a greater understanding of the emission processes in such lasers will have relevance to the spatial and temporal profiles in all optically emitting semiconductor diodes, including continuous-wave lasers and light-emitting diodes (LEDs).

INPUT–OUTPUT CHARACTERISTICS OF PASSIVELY *Q*-SWITCHED LASERS

The dependence of cavity losses of these lasers under different implantation dosages was studied. Both facets of the laser were implanted by a dose of O^{3+} ions of 17 MeV energy, accelerated by a cyclotron. Equal doses of ions were applied to both facets.

In order to examine the behavior of the ion-implanted lasers, it was necessary to study the losses of these lasers prior to ion implantation. This was done by studying the threshold current for different cavity lengths, since the external cavity loss is given by

$$\alpha_{\text{out}}=\frac{1}{2L}\ln\left(\frac{1}{R_1R_2}\right), \tag{1}$$

where R is the cavity reflection coefficient and L is the cavity length. There is a linear dependence of the threshold current density, J_{th}, versus absorption, which fits the relationship:

$$J_{\text{th}}(\text{kA cm}^{-2})=7.2\times10^{-2}\alpha_{\text{out}}(\text{cm}^{-1})+1.8. \tag{2}$$

It is this simple relationship between threshold current density and losses that allows the determination of laser cavity losses after ion implantation. The laser output optical power versus pumping current characteristics for varying implantation dosages were measured. These input–output characteristics measured under direct current electrical pumping are shown in Fig. 1. In each case, these input–output characteristics are shown for increasing current, since some hysteresis was exhibited. Figure 1(b) explains how the saturated and unsaturated threshold currents, I_{th} and I'_{th}, respectively, were taken for the calculations. Figure 1(a) shows a clear increase in the laser threshold current with increasing ion dosage, and this is plotted in Fig. 2(a). In addition, Figure 1(a) shows an increase in the gradient of the curve after lasing with increasing ion dosage, which indicates a reduction in the laser differential quantum efficiency caused by ion implantation. This is further illustrated in Fig. 2(b).

We can assume that the near-vertical part of the characteristic for the ion-implanted lasers is due to saturation of absorption within the implanted regions, caused by the dynamic Moss–Burstein shift.[6,7] This region is formed by the tracks of the heavy ions during implantation, and in this case is estimated to be 10 μm in depth.[4] Assuming that the losses in the saturable absorber are a component of the increased ''new'' output losses α^*_{out}, and given the experimental dependence of threshold current on output losses [shown in Eq. (2)], we can obtain from Eq. (1)

$$J'_{\text{th}}(\text{kA cm}^{-2})=7.2\times10^{-2}\times\frac{1}{2L}\ln\left(\frac{1}{R'_1R'_2}\right)(\text{cm}^{-1})+1.8, \tag{3}$$

a)Electronic mail: G.S.Buller@hw.ac.uk

 © 1998 American Institute of Physics

Downloaded 30 Jan 2002 to 137.195.29.233. Redistribution subject to AIP license or copyright, see http://ojps.aip.org/japo/japcr.jsp

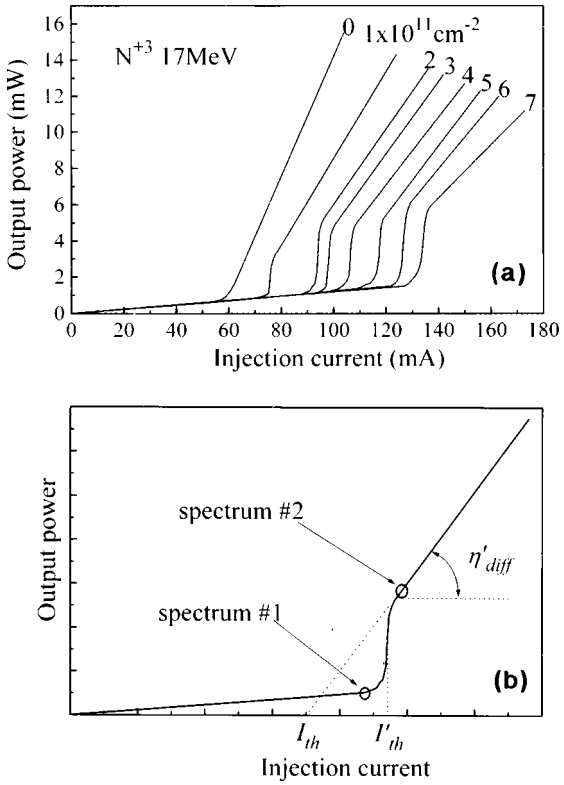

FIG. 1. (a) Plot of optical output power vs injection current for a laser with ion implantations of 0, 1, 2, 3, 4, 5, 6, and 7×10^{11} cm^{-2}. (b) Schematic representation of the terms used in describing the continuous-wave laser characteristics.

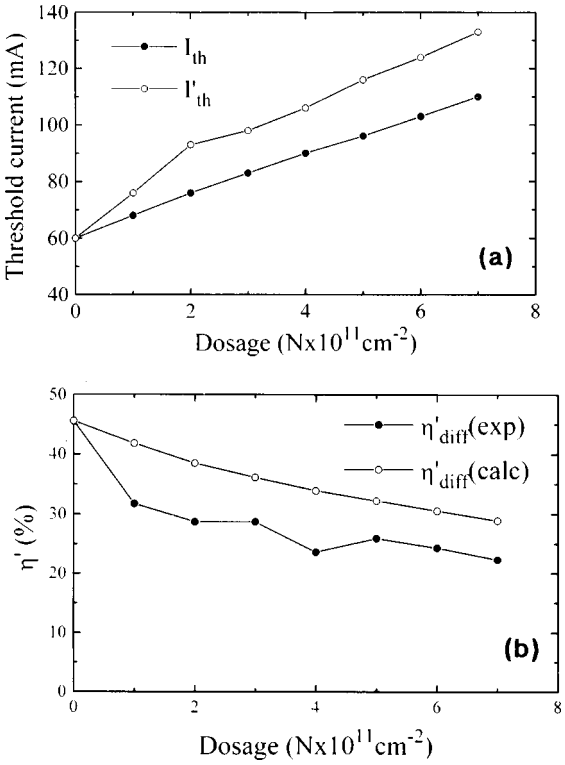

FIG. 2. (a) Laser threshold current vs ion dosage for the same laser described in Fig. 1. (b) Plot of differential quantum efficiency, η'_{diff}, vs dosage for the same laser.

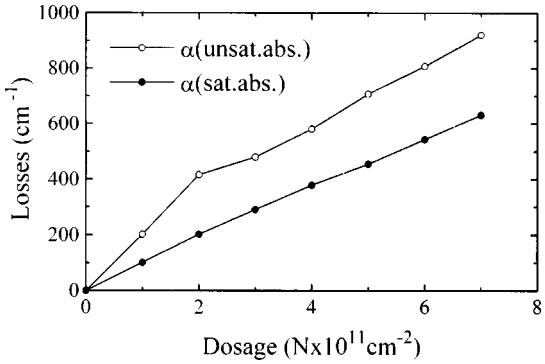

FIG. 3. Distributed modal losses for saturated and nonsaturated regimes in the saturable absorber for various ion implantation dosages, calculated from data of Fig. 1.

where $R'_{1,2}$ is the reflectivity of the cavity after ion implantation. Given the cavity length and supposing $R'_1=R'_2$ and $R_1=R_2$, we can calculate the reflectivities from the data presented in Fig. 2(a).

From the initial value of the reflection coefficient and the length of the saturable absorber region, it is possible to plot the saturable absorber modal losses for both states of the absorber. This dependence is shown in Fig. 3. It should be noted that the nonsaturated state absorption is a lower limit, since the absorption coefficient will be slightly higher for lower optical excitation. Because the optical confinement factor for a laser mode in the active region of double heterostructure lasers will not usually exceed 0.5, the corresponding nonsaturated material losses are at least twice as high as the modal losses shown in Fig. 3.

The value of the modal loss in the saturated case is proportional to the ion implantation dose and must coincide with material losses. These losses are caused by defects in the crystal structure formed by ion implantation and play a major role in the reduction of the differential quantum efficiency, η'_{diff}. The defect density is expected be proportional to the ion dose over a wide range of implantation conditions. The upper limit of the η'_{diff} may be estimated by using following formula:

$$\eta'_{\text{diff}}=\alpha_{\text{out}}/(\alpha'_{\text{out}}+\alpha_{\text{int}}), \tag{4}$$

where α_{out} is the initial output loss calculated from Eq. (1), α'_{out} is the saturated loss from Fig. 3 which contains material loss and basic output loss (e.g., from mirrors), and α_{int} is the distributed loss of the laser waveguide in the lasing regime. The results of these calculations are compared with the experimental results in Fig. 2(b). Some difference between experiment and these simulations can be explained by the longitudinal leakage of carriers towards the absorber regions, which serves to reduce η'_{diff}, however the magnitude of this effect is difficult to estimate.

Spectral analysis of the laser output was also performed. Two spectra, measured at currents below and above the ''vertical'' part of the input–output characteristic, as illustrated in Fig. 1(b), are shown in Fig. 4. The pumping current was taken as close as possible to a vertical part of the curve. These spectra clearly show a sharp transition from the spontaneous recombination regime to lasing via the saturation of

Downloaded 30 Jan 2002 to 137.195.29.233. Redistribution subject to AIP license or copyright, see http://ojps.aip.org/japo/japcr.jsp

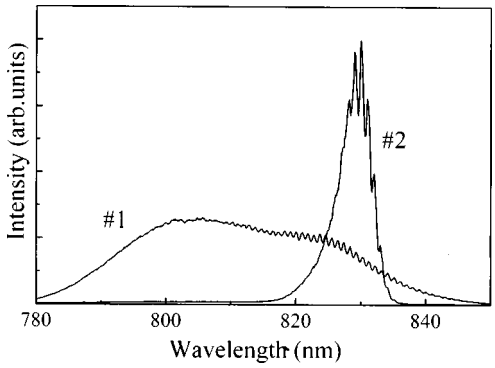

FIG. 4. Spectral output of the device below and above laser threshold as described in Fig. 1(b).

absorber. Lasing at currents below the vertical part of the curve was not observed. The maximum power of the spontaneous emission was observed to be approximately 1.5 mW.

DYNAMIC OUTPUT PROPERTIES

In order to study the evolution of the lasing pulse over a wide dynamic range, the pulsed emission was measured using the time-correlated single-photon counting technique.[8] In these experiments a Si single-photon avalanche diode (SPAD) detector[9,10] with an active area diameter of $\sim 7\ \mu$m was used, and this allows an instrumental response of <50 ps (full width at half maximum). An active quenching circuit (AQC) was utilized in order to fully exploit the performance of the detectors.[10] Among the advantages of this type of detection system are the high photon detection efficiency and the large timing dynamic range (ps–μs). This type of detector has been used, for example, in measurements of time-resolved photoluminescence from semiconductors[11] and in time-of-flight profiling experiments.[12] Examples of the time-resolved emission characteristics for a 830 nm wavelength laser are shown on a semilogarithmic plot in Fig. 5. In Fig. 5, time-resolved characteristics at the laser wavelength band (in this case, measured between 825 and 835 nm) and at wavelengths greater than the laser wavelength (845–855 nm) were measured. It should be noted that both curves are normalized to the same peak height by the use of different acquisition times and rates, and hence no significance should be given to the relative amplitudes. The lasing wavelength emission indicates a rapid increase in intensity, approximately three orders of magnitude, in $\sim$100 ps. The longer wavelength emission, however, indicates a much slower rise in intensity, corresponding roughly to the application of the electrical input pulse. This is consistent with spontaneous emission, corresponding with the increase of nonequilibrium carrier concentration. The longer wavelength emission can be subdivided into three parts: (i) first, an increase that is in proportion to the carrier concentration; (ii) second, an exponential rise which corresponds with superluminescence in a cavity with significant losses; and (iii) a small decrease in the spontaneous emission, occurring at the point of saturation of the implanted region, which subsequently leads to laser *Q*-switching. The results of Fig. 5 show that no lasing is observed before the saturation of the absorber, and that the origin of the *Q*-switching is likely caused by the saturation of the absorber by superluminescence emitted from the gain region. The slow decay observed just after the peak on the 830 nm emission originates from the slow tail observed in this particular type of single-photon detector used,[9] and is not caused by the emission processes of the laser (this is confirmed by independent streak camera measurements on the same laser).

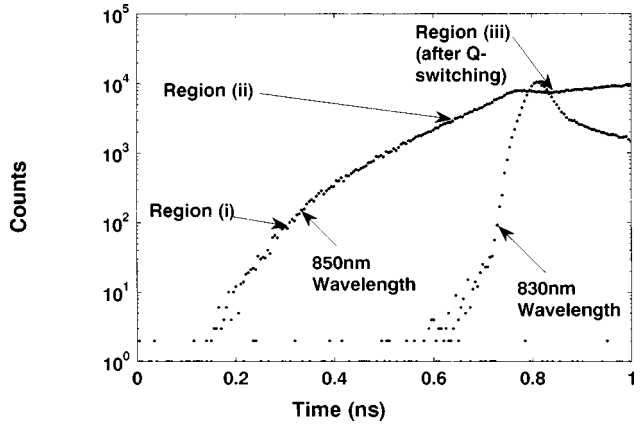

FIG. 5. Time-resolved emission from the 830 nm laser displayed on a semilogarithmic plot for (a) the lasing wavelength band at 825–835 nm and (b) the wavelength band at 845–855 nm.

DISCUSSION

In order to estimate the maximum level of spontaneous emission from the laser, which will not saturate the absorber, measurements were performed to investigate the radiation emitted from a laser implanted into only one facet. When pumped by short electrical pulses (duration $\sim$2 ns), this device demonstrated lasing in the *Q*-switching regime. Therefore, spontaneous radiation is emitted via the nonimplanted facet without loss in that direction. The transition to the saturated regime occurred at approximately an average optical power of 5 mW (integrated over the pulse duration) when measured from the nonimplanted facet of the laser. This optical power gives an indication of the optical irradiance necessary to influence saturation of the ion-implanted region, which in this particular case is at the other facet of the laser. Previous studies[5,13] have indicated that the lifetime of nonequilibrium carriers in the ion-implanted region is a few picoseconds. This estimate is in agreement with observations of intracavity mode locking in these lasers,[13,14] which requires the carrier lifetime in the saturable absorber to be comparable to or less than the roundtrip period of the laser, which is less than 5 ps for the length of cavity used in these measurements.

The saturation of the optical losses in the ion-implanted layer is caused by the Moss–Burstein shift of the absorption edge due to the rising carrier concentration. This increase in carrier concentration can only be caused by absorption of radiation from the active section of the laser. However, if we assume the carrier lifetime within the ion-implanted region is τ, and optical excitation power is P, then the carrier concentration, N, within the absorbing region is given by

Downloaded 30 Jan 2002 to 137.195.29.233. Redistribution subject to AIP license or copyright, see http://ojps.aip.org/japo/japcr.jsp

$$N=\frac{P\tau\lambda\Gamma}{hcAl}, \tag{5}$$

assuming all the light is absorbed within the saturable absorber section. Here A is the cross-sectional area of the gain region, Γ is the confinement factor (estimated at 0.5), l is the length of the saturable absorber, c is the speed of light, and h in Planck's constant. If we assume typical values of $l=10\ \mu$m, $A=1\ \mu\text{m}^2$, $\tau\leqslant 5$ ps for a 800 nm wavelength laser, then the carrier concentration within the saturable absorber for a constant power input of 5 mW is only $\sim 5\times 10^{15}\ \text{cm}^{-3}$. However, for a sufficient shift of the absorption edge of the implanted region for lasing to occur, there must be a photo-induced carrier concentration of at least $5\times 10^{17}\ \text{cm}^{-3}$.[6,7] This absorption edge shift should provide a significant reduction in optical loss at the gain wavelength spectral region, which is based on the same materials as the saturable absorber.

If we assume that the threshold current is ~300 mA and that the lifetime in the active region is not less than 100 ps, then, given the volume of the active region, the nonequilibrium carrier concentration is not less than $3\times 10^{18}\ \text{cm}^{-3}$. The luminescence from GaAs with such a high concentration of nonequilibrium carriers was observed for the first time in 1962 and was called ''superluminescence.'' This nonequilibrium carrier concentration corresponds to a distance between carriers of as little as 10 nm. However, a fundamental requirement of the Einstein theory of stimulated emission is that the distance between dipoles must be much greater than the emitting wavelength, which is ~200 nm in this case. Assuming the above carrier density, there must be $>2\times 10^{-1}$ nonequilibrium carriers in a cube with sides equal to one wavelength, which is clearly a strong transgression of the Einstein description of this process. It is known, however, that such a transgression in solid-state lasers leads to bursts of coherent radiation, known as Dicke superradiation.[15] The parameters of the optical pulses depend on the number of dipoles involved in the collective resonance. In solid-state lasers, the coherent pulses are relatively long and straightforward to examine. However, estimates of the pulse parameters for semiconductor heterostructures[16] for these collective radiation effects show that the optical pulses are less than 1 ps in duration and less than 1 pJ.

It was recently shown by optical autocorrelation studies of superluminescence in semiconductor material that a high concentration of nonequilibrium carriers appears to lead to the formation of very short pulses of the coherent radiation.[17–19] These experiments used a GaAs two-photon absorption detector in an autocorrelation configuration to measure bursts of radiation from InGaAsP/InP lasers emitting at $\lambda=1.3\ \mu$m with subpicosecond temporal resolution. It was found that pulses of $\leqslant 1$ ps duration were emitted when the lasers were operated with continuous electrical pumping. The existence of such pulses could be an explanation of the nature of the origin of the dynamic Moss–Burstein shift of the absorption edge in ultrafast saturable absorbers formed by the heavy ion implantation and the subsequent Q-switching of semiconductor lasers fabricated with such absorbers.

CONCLUSIONS

Studies of the current density threshold and the differential quantum efficiency in ion-implanted passively Q-switched lasers in conjunction with high-sensitivity measurements of the laser pulse temporal profile have shown that the initiation of the laser pulse is unlikely to be caused by mode locking or spontaneous emission. Recent results examining stimulated collective radiation effects in similar semiconductor materials have offered a potential explanation for the origin of the passive Q-switching in such lasers.

[1] J. P. Van der Ziel, W. T. Tsang, R. A. Logan, R. M. Mikulyak, and W. M. Augustyniak, Appl. Phys. Lett. **39**, 525 (1981).
[2] N. Stelmakh and J. M. Lourtioz, Electron. Lett. **29**, 160 (1993).
[3] Zh. I. Alferov, A. B. Zhuralev, E. L. Portnoi, and N. M. Stel'makh, Sov. Tech. Phys. Lett. **12**, 452 (1986).
[4] E. L. Portnoy, E. A. Avrutin, and A. V. Chelnokov, *Nonlinear Effects in Picosecond High-Power Lasers*, Proceedings of the Soviet-American Workshop on the Physics of Semiconductor Lasers, 1991 AIP Conf. Proc. No. 240 (AIP, New York, 1991), pp. 58–67.
[5] A. B. Zhuralev, V. A. Marushchak, E. L. Portnoi, N. M. Stel'makh, and A. N. Titkov, Sov. Phys. Semicond. **22**, 217 (1988).
[6] See, for example, *Optical Bistability: Controlling Light with Light*, edited by H. M. Gibbs (Academic, New York, 1985).
[7] D. A. B. Miller, Laser Focus **19**, 61 (1982).
[8] See, for example, D. V. O'Connor and D. Phillips, *Time-correlated Single-photon Counting* (Academic, New York, 1983).
[9] S. Cova, A. Lacaita, M. Ghioni, G. Ripamonti, and T. A. Louis, Rev. Sci. Instrum. **60**, 1104 (1989).
[10] S. Cova, M. Ghioni, A. Lacaita, C. Samori, and F. Zappa, Appl. Opt. **35**, 1956 (1996).
[11] G. S. Buller, J. S. Massa, and A. C. Walker, Rev. Sci. Instrum. **63**, 2994 (1992).
[12] J. S. Massa, A. M. Wallace, G. S. Buller, S. J. Fancey, and A. C. Walker, Opt. Lett. **22**, 543 (1997).
[13] E. M. Dianov, A. B. Grudinin, I. Yu. Krushchev, D. V. Kuksenkov, E. L. Portnoy, and S. V. Zaitsev, Sov. Lightwave Commun. **2**, 31 (1992).
[14] E. L. Portnoy and A. V. Chelnokov, IEEE International Conference on Semiconductor Lasers, Davos Switzerland, 1990.
[15] R. H. Dicke, Phys. Rev. **93**, 99 (1954).
[16] L. Allen and J. H. Eberly, *Optical Resonance and Two-level Atoms* (Wiley, New York, 1975).
[17] S. V. Zaitsev and A. M. Georgievski, International Conference on Optical Diagnostics of Materials and Devices for Opto-, Micro-, and Quantum Electronics (OPTDIM '95/SPIE), Kiev, Ukraine, May 1995, SPIE Proceedings, Vol. 2648-50, pp. 319–324.
[18] A. M. Georgievski and S. V. Zaitsev, Instrum. Exp. Tech. **39**, 132 (1996).
[19] S. V. Zaitsev and A. M. Georgievski, *Proceedings of the International Conference QDS'96, Sapporo*, Japan, 4–7 November 1996 [Jpn. J. Appl. Phys., Part 1 **36**, 4209 (1997)].

Downloaded 30 Jan 2002 to 137.195.29.233. Redistribution subject to AIP license or copyright, see http://ojps.aip.org/japo/japcr.jsp